Experimental analysis of emission linewidth narrowing in a pulsed $KGd(WO_4)_2$ Raman laser

Vasili G. Savitski*

Institute of Photonics, University of Strathclyde, Wolfson Centre, 106 Rottenrow, Glasgow G4 0NW, UK
**vasili.savitski@strath.ac.uk*

Abstract: The linewidth of a $KGd(WO_4)_2$ (KGW) intracavity pumped Raman laser is analyzed experimentally for different configurations of the Raman and pump laser resonators: with narrow and broadband pump emission profiles, with and without linewidth narrowing elements in the Raman laser resonator, with and without injection seeding into the Raman cavity. The benefits of a narrow linewidth pump source in combination with linewidth narrowing elements in the Raman laser cavity for the efficient linewidth narrowing of the Raman laser emission are explained. 20 kW peak-power pulses at 1156 nm with 0.43 cm^{-1} emission linewidth are demonstrated from an injection seeded KGW Raman laser.

OCIS codes: (140.3540) Lasers, Q-switched; (140.3550) Lasers, Raman; (140.3580) Lasers, solid-state.

References and links

1. J. Dakin and R. G. W. Brown, *Handbook of optoelectronics*, (Taylor & Francis, 2006).
2. M.-C. Amann, T. M. Bosch, M. Lescure, R. A. Myllylae, and M. Rioux, "Laser ranging: a critical review of unusual techniques for distance measurement," Opt. Eng. **40**(1), 10–19 (2001).
3. G. L. Clark and E. D. Harris, *High Power Laser Amplifier Chain Techniques* (Defense Technical Information Center, 1965).
4. R. Nicolaescu, E. S. Fry, and T. Walther, "Generation of near-Fourier-transform-limited high-energy pulses in a chain of fiber-bulk amplifiers," Opt. Lett. **26**(1), 13–15 (2001).
5. Z. Renjie, S. Wei, E. Petersen, A. Chavez-Pirson, M. Stephen, and N. Peyghambarian, "Transform-limited, injection seeded, Q-switched, ring cavity fiber laser," J. Lightwave Technol. **30**(16), 2589–2595 (2012).
6. E. J. Woodbury and W. K. Ng, "Ruby laser operation in near IR," Proc. IRE **50**(11), 2367 (1962).
7. J. C. White and D. Henderson, "Anti-Stokes Raman laser," Phys. Rev. A **25**(2), 1226–1229 (1982).
8. J. N. Holliday, "Design of a XeF-pumped second Stokes amplifier for blue-green production in H_2," Opt. Lett. **8**(1), 12–14 (1983).
9. G. M. A. Gad, H. J. Eichler, and A. A. Kaminskii, "Highly efficient 1.3-μm second-Stokes $PbWO_4$ Raman laser," Opt. Lett. **28**(6), 426–428 (2003).
10. V. I. Dashkevich, V. A. Orlovich, and A. P. Shkadarevich, "Intracavity Raman laser generating a third stokes component at 1.5 μm," J. Appl. Spectrosc. **76**(5), 685–691 (2009).
11. H. Zhu, Y. Duan, G. Zhang, C. Huang, Y. Wei, H. Shen, Y. Zheng, L. Huang, and Z. Chen, "Efficient second harmonic generation of double-end diffusion-bonded Nd:YVO_4 self-Raman laser producing 7.9 W yellow light," Opt. Express **17**(24), 21544–21550 (2009).
12. V. I. Dashkevich and V. A. Orlovich, "Ring solid-state Raman laser at 1538 nm," Laser Phys. Lett. **8**(9), 661–667 (2011).
13. W. Lubeigt, V. G. Savitski, G. M. Bonner, S. L. Geoghegan, I. Friel, J. E. Hastie, M. D. Dawson, D. Burns, and A. J. Kemp, "1.6 W continuous-wave Raman laser using low-loss synthetic diamond," Opt. Express **19**(7), 6938–6944 (2011).
14. V. G. Savitski, I. Friel, J. E. Hastie, M. D. Dawson, D. Burns, and A. J. Kemp, "Characterization of single-crystal synthetic diamond for multi-watt continuous-wave Raman lasers," IEEE J. Quantum Electron. **48**(3), 328–337 (2012).
15. G. M. Bonner, J. Lin, A. J. Kemp, J. Wang, H. Zhang, D. J. Spence, and H. M. Pask, "Spectral broadening in continuous-wave intracavity Raman lasers," Opt. Express **22**(7), 7492–7502 (2014).
16. K. V. Yumashev, V. G. Savitski, N. V. Kuleshov, A. A. Pavlyuk, D. D. Molotkov, and A. L. Protasenya, "Laser performance of N_g-cut flash-lamp pumped Nd:KGW at high repetition rates," Appl. Phys. B **89**(1), 39–43 (2007).
17. P. A. Loiko, V. E. Kisel, N. V. Kondratuk, K. V. Yumashev, N. V. Kuleshov, and A. A. Pavlyuk, "14 W high-efficiency diode-pumped cw Yb:$KGd(WO_4)_2$ laser with low thermo-optic aberrations," Opt. Mater. **35**(3), 582–585 (2013).

#216576 - $15.00 USD Received 7 Jul 2014; revised 15 Aug 2014; accepted 17 Aug 2014; published 2 Sep 2014

18. N. V. Kravtsov, N. I. Naumkin, and V. P. Protasov, "Characteristics of the dynamics of stimulated Raman scattering in a gas excited by a train of short pulses," Sov. J. Quantum Electron. **5**(7), 864–865 (1975).
19. Y. B. Band, J. R. Ackerhalt, J. S. Krasinski, and D. F. Heller, "Intracavity Raman lasers," IEEE J. Quantum Electron. **25**(2), 208–213 (1989).
20. H. M. Pask, "Continuous-wave, all-solid-state, intracavity Raman laser," Opt. Lett. **30**(18), 2454–2456 (2005).
21. C. V. Raman and K. S. Krishnan, "A new type of secondary radiation," Nature **121**(3048), 501–502 (1928).
22. N. Hodgson and H. Weber, *Laser Resonators and Beam Propagation. Fundamentals, Advanced Concepts, Applications* (Springer-Verlag, 2005).
23. L. E. Erickson and A. Szabo, "Spectral narrowing of dye laser output by injection of monochromatic radiation into the laser cavity," Appl. Phys. Lett. **18**(10), 433–435 (1971).
24. N. P. Barnes and B. M. Walsh, "Amplified spontaneous emission-application to Nd:YAG lasers," IEEE J. Quantum Electron. **35**(1), 101–109 (1999).
25. P. Bado, M. Bouvier, and J. S. Coe, "Nd:YLF mode-locked oscillator and regenerative amplifier," Opt. Lett. **12**(5), 319–321 (1987).
26. P. A. Schulz and S. R. Henion, "5-GHz mode locking of a Nd:YLF laser," Opt. Lett. **16**(19), 1502–1504 (1991).
27. D. J. Spence, P. Dekker, and H. M. Pask, "Modeling of continuous wave intracavity Raman lasers," IEEE J. Sel. Top. Quantum Electron. **13**(3), 756–763 (2007).
28. A. Penzkofer, A. Laubereau, and W. Kaiser, "High-intensity Raman interactions," Prog. Quantum Electron. **6**(2), 55–140 (1979).
29. C.-S. Wang, "Theory of stimulated Raman scattering," Phys. Rev. **182**(2), 482–494 (1969).
30. M. G. Raymer and J. Mostowski, "Stimulated Raman scattering: unified treatment of spontaneous initiation and spatial propagation," Phys. Rev. A **24**(4), 1980–1993 (1981).
31. V. A. Chirkov, V. S. Gorelik, G. V. Peregudov, and M. M. Sushchinskii, "Investigation of the line width of stimulated Raman scattering," JETP Lett. **10**(9), 267–269 (1969).
32. L. Fan, Y.-X. Fan, Y.-Q. Li, H. Zhang, Q. Wang, J. Wang, and H.-T. Wang, "High-efficiency continuous-wave Raman conversion with a $BaWO_4$ Raman crystal," Opt. Lett. **34**(11), 1687–1689 (2009).
33. T. T. Basiev, A. A. Sobol, P. G. Zverev, V. V. Osiko, and R. C. Powell, "Comparative spontaneous Raman spectroscopy of crystals for Raman lasers," Appl. Opt. **38**(3), 594–598 (1999).

1. Introduction

High average power pulsed lasers with a narrow (ideally – transform-limited) emission linewidth are essential for LIDAR (LIght Detection And Ranging) applications [1,2]. For LIDAR, better range and velocity resolution require shorter pulses and narrower emission linewidths respectively [1]. Simultaneous shortening of laser pulse duration and narrowing of the corresponding emission linewidth require generation of transform-limited pulses. A system with a high signal to noise ratio requires high average power [1], and, hence, high pulse energies or repetition rates. Higher pulse energies are usually preferable since a high repetition rate limits the range of the LIDAR system [1].

Narrow linewidth high power lasers suitable for LIDAR applications are usually based on fiber master oscillator power amplifier (MOPA) technology [3–5]. On the other hand, conversion of the pump wavelength via stimulated Raman scattering (SRS) [6] in crystalline media adds more flexibility in terms of output wavelength [7–14]. However, less work has been reported on emission linewidth narrowing in solid-state (non-fiber) Raman lasers. To the best of our knowledge there is no research targeting Raman linewidth narrowing in solid-state Raman lasers emitting in pulsed regime. Only recently, the effect of broadening of the fundamental emission linewidth on the effective Raman gain in Raman lasers was studied [15].

In this paper report a proof of concept demonstration of a narrow linewidth crystalline Raman laser operating in pulsed mode with high peak power is reported. The effect of narrow linewidth injection seeding at the Raman laser wavelength on the performance of the Raman laser is studied.

2. Experimental setup

The Raman laser was built around an N_g-cut $KGd(WO_4)_2$ (KGW) crystal, giving a positive thermal lens [16,17] which simplifies the Raman laser cavity design. The crystal was 30 mm in length. The end faces were anti-reflection (AR) coated for 1 and 1.15 μm (R<0.1%). The source of fundamental laser emission was a diode side-pumped Nd:$LiYF_4$ (Nd:YLF) module emitting at 1047 nm and described in detail in [14]. The Raman shift of 901 cm^{-1} (which corresponds to a shift of the fundamental wavelength from 1047 nm to 1156 nm) was selected

#216576 - $15.00 USD Received 7 Jul 2014; revised 15 Aug 2014; accepted 17 Aug 2014; published 2 Sep 2014

by appropriate choice of the coatings of Raman laser mirrors. An intracavity Raman laser configuration [18–20], shown in Fig. 1(a), for wavelength conversion from 1 to 1.15 μm was chosen.

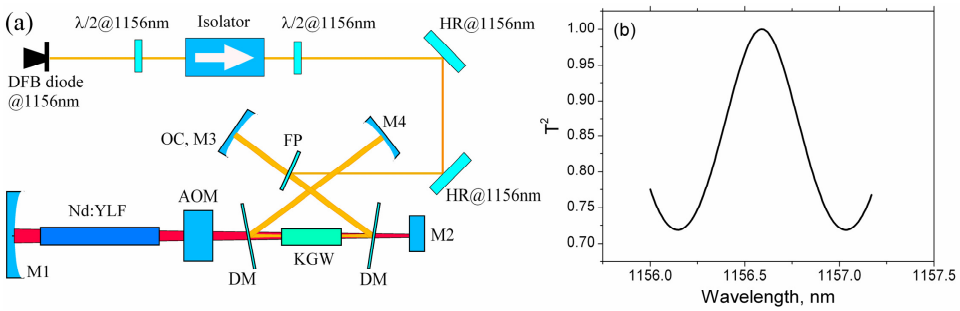

Fig. 1. (a) The KGW Raman laser set-up. M1: HR@1047 nm, ROC = 500 mm; M2: plane, HR@1047 nm or VBG; M3: R@1156 nm 81%, ROC = 200 mm; M4: HR@1156 nm, ROC = 250 mm; DM: HR@1156 nm, HT@1047 nm; FP: Fabry-Perot etalon. (b) Calculated double-pass transmittance (T^2) of the FP as a function of wavelength at the angle of incidence of 7°.

The cavities of the Nd:YLF laser and the KGW Raman laser were coupled using dichroic mirrors (DM: highly reflective (HR) at 1.1-1.25 μm, highly transmissive (HT) at 1 μm). Mirrors M1 (radius of curvature (ROC) 500 mm, HR at 1 μm) and M2 (plane, either HR at 1 μm or a Volume Bragg Grating (VBG, OptiGrate)) formed the cavity of the Nd:YLF laser, as shown in Fig. 1(a). The KGW Raman laser cavity was formed by the output coupler M3 (ROC 200 mm, reflectivity of 81% at 1.15 μm), dichroic mirrors DM and mirror M4 (ROC 250 mm, HR at 1.15 μm). The KGW crystal was wrapped into indium foil and mounted in a brass mount. No water-cooling was provided to the crystal.

The Nd:YLF laser cavity was designed to be stable against a thermal lens in the Nd:YLF rod with a focal length of ~-150 mm or longer (the manufacturer specifies a focal length of –750 mm at maximum diode pump power), and, simultaneously, against a thermal lens in the KGW of 200 mm focal length or longer. The thermal lens in the KGW crystal results from the inelastic nature of Raman scattering [21]. Our calculations indicate that the main factor, influencing the fundamental (TEM_{00}) mode size of 1047 nm field in the Nd:YLF and KGW crystals is the thermal lens in the KGW. When the focal length of the thermal lens in the KGW crystal increases from 200 to 1000 mm, the TEM_{00} beam radius of the 1047 nm field increases from 190 to 345 μm in the Nd:YLF and decreases from 375 to 345 μm in the KGW. The TEM_{00} beam radii of the 1156 nm field in the KGW crystal varies from 213 to 203 μm when the focal length of thermal lens in the KGW crystal increases from 200 to 1000 mm.

The acousto-optic Q-switch (AOM) was 50 mm long and its faces were AR coated for 1047 nm (R<0.2%). The VBG had reflectivity of 99.9% at the central wavelength of 1047.4 nm and reflectivity linewidth at full-width half-maximum (FMHW) of 0.29 nm. A 0.5 mm thick fused-silica Fabry-Perot (FP) etalon was inserted into the KGW Raman cavity during the experiments on linewidth narrowing. Its angle with respect to the cavity axis was ~7° and was finely tuned to maximise the Raman laser output power. Transmittance of the etalon as a function of wavelength after double passing of the laser beam (T^2), calculated using the equation in [22] is shown in Fig. 1(b).

The narrow linewidth (<4 MHz FWHM) distributed-feedback (DFB) laser diode (Toptica photonics) emitted a single transverse and longitudinal mode at 1156.6 nm and was used to injection-seed [23] the Raman laser via the reflection from the Fabry-Perot etalon. It has a maximum power of 12 mW (being attenuated down to 3 mW after passing through the isolator and waveplates, see Fig. 1(a)), and could be tuned from 1155 to 1157 nm. Emission from this laser diode was launched into the Raman cavity via an optical isolator. Injection seeding was not attempted without the FP etalon as it provided the only way to inject the seed emission into the Raman cavity. Despite the fact that the calculated transmittance peak of the

#216576 - $15.00 USD Received 7 Jul 2014; revised 15 Aug 2014; accepted 17 Aug 2014; published 2 Sep 2014

FP etalon is at 1156.6 nm [Fig. 1(a)], about 2% of the seed emission could still be injected into the Raman cavity thanks to some divergence of the beam.

Emission spectra were measured by the optical spectrum analyzer (OSA, Agilent 86142B). The FWHM linewidth of the seed emission was measured to be $\Delta\nu_R$ = 0.06 nm (0.45 cm^{-1}) and is instrument-limited by the spectral resolution of the OSA. Therefore, the FWHM linewidths $\Delta\nu$ of the Raman and fundamental (1047 nm) emission presented below are obtained after deconvolution of the measured values $\Delta\nu_m$: $\Delta\nu = \sqrt{\Delta\nu_m^2 - \Delta\nu_R^2}$, taking into account Gaussian shapes of the instrument-limited response and measured spectra.

3. Experimental results

The Q-switching repetition rate (frequency) of the Nd:YLF laser giving the highest Raman laser pulse energy was assessed first. The output pulses energies at 1047 nm and 1156 nm were measured for repetition rates between 1 and 10 kHz. The output at 1047 nm was measured without the KGW crystal in the cavity and with an output coupler reflectivity of 80% (mirror M2 in Fig. 1(a)). The output at 1156 nm was measured with the M2 mirror being HR@1047nm. The Raman laser pulse energy was maximized at a Q-switching frequency of 2 kHz, as shown in Fig. 2. All the results presented below were obtained at this frequency. The reduced pulse energy of the Nd:YLF laser at frequencies below ~3 kHz is probably due to either amplified spontaneous emission or parasitic lasing [24].

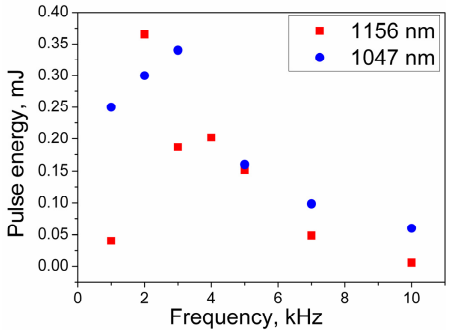

Fig. 2. Output energies of fundamental (1047 nm) and Raman (1156 nm) lasers as a function of Q-switching frequency.

The performance of the KGW Raman laser was analyzed in five configurations:

i) No linewidth control of the fundamental or Raman emission (VBG-, FP-);

ii) Fundamental emission linewidth control with a VBG, no Raman emission linewidth narrowing (VBG + , FP-);

iii) No fundamental emission linewidth control, Raman emission linewidth control with an intracavity etalon (VBG-, FP +);

iv) Linewidth control of both the fundamental and Raman emission (VBG + , FP +);

v) Linewidth control of both the fundamental and Raman emission (VBG + , FP +), with additional injection seeding of the Raman laser.

The average output power of the KGW Raman laser as a function of diode pump power launched into the Nd:YLF laser module is shown in Fig. 3(a) for all 5 configurations. The highest output power of 1500 mW (pulse energy of 0.75 mJ) was observed for configuration i) (VBG-, FP-). Optical damage of the dichroic mirrors, which occurred at Raman output energies of ~0.7-0.75 mJ, prevented any further increase in output power. The slope efficiencies of the Raman laser with respect to incident diode laser pump power were estimated 3.3, 3.3, 3, 2.4, and 2.4% for Raman laser configurations i) to v) respectively. These values are lower than for systems based on end-pumped neodymium lasers due to the side-

#216576 - $15.00 USD Received 7 Jul 2014; revised 15 Aug 2014; accepted 17 Aug 2014; published 2 Sep 2014

pumping scheme of the Nd:YLF laser system used in this study. The corresponding Raman laser thresholds were 26, 35, 36, 35 and 33 W. It should be noticed that the values of the diode pump powers are given based on the manufacturer's calibration of the diode pump power w.r.t. diode current, and could be slightly lower due to the ageing effect of the diodes. The output power of the KGW Raman laser in configuration v), with injection seeding, was consistently higher than that in configuration iv) (i.e. with the same linewidth narrowing elements but without injection seeding).

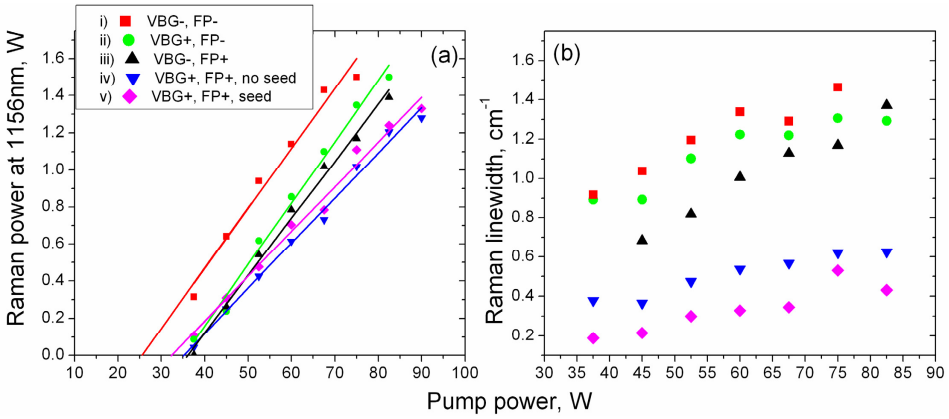

Fig. 3. Raman laser output power (a) and linewidths of theRaman laser emission (b) as functions of diode incident pump power for different cavity configurations.

The linewidth of the 1156 nm emission monotonically decreased in moving from configuration i) to v), as shown in Fig. 3(b). The minimum Raman emission linewidth at the maximum pump power of 82.5 W was 0.06 nm (0.43 cm^{-1}) for configuration v) with injection seeding. The corresponding Raman laser average output power was 1.33 W (pulse energy 0.67 mJ). This Raman laser linewidth was about 30% narrower in comparison with the one measured for laser configuration iv), i.e. without injection seeding. Moreover, as it was already mentioned above, with the injection seeding the output power was higher (for ~5%) than that in configuration iv) within the entire pump power range.

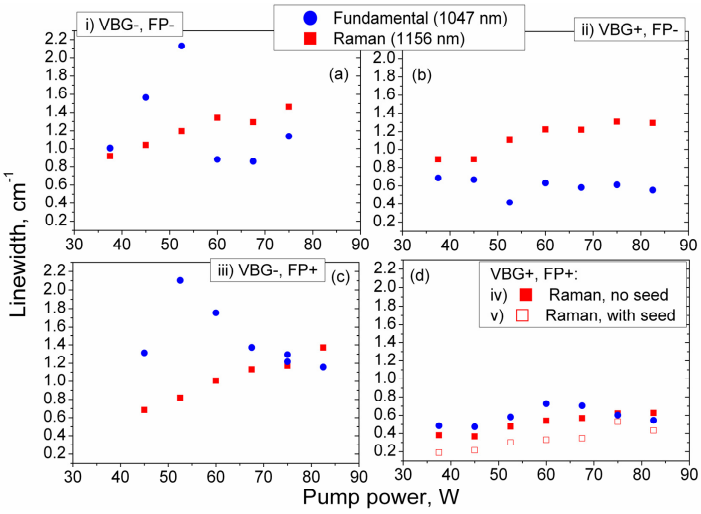

Fig. 4. Linewidths of fundamental and Raman laser emissions as function of incident diode pump power for different cavity configurations.

#216576 - $15.00 USD Received 7 Jul 2014; revised 15 Aug 2014; accepted 17 Aug 2014; published 2 Sep 2014

The 1156 nm Raman linewidth measurements together with those of the fundamental emission at 1047 nm are presented in Fig. 4. When no special narrowing elements are put in both fundamental and Raman laser cavities, the Raman laser emission linewidth at Raman threshold is close to that of the fundamental emission [Fig. 4(a)]. The presence of the VBG in the fundamental laser cavity narrows the 1047 nm linewidth, as shown in Fig. 4(b). Raman emission linewidth demonstrates some narrowing with the FP element in the Raman resonator [Fig. 4(c)], but substantial narrowing of the Raman emission linewidth is observed only in configurations iv) and v) [Fig. 4(d)], when linewidth narrowing elements are present in both the fundamental and Raman laser cavities. The fundamental laser emission linewidth at 1047 nm for configuration v) (VBG + , FP + , with seed) was identical to that for configuration iv).

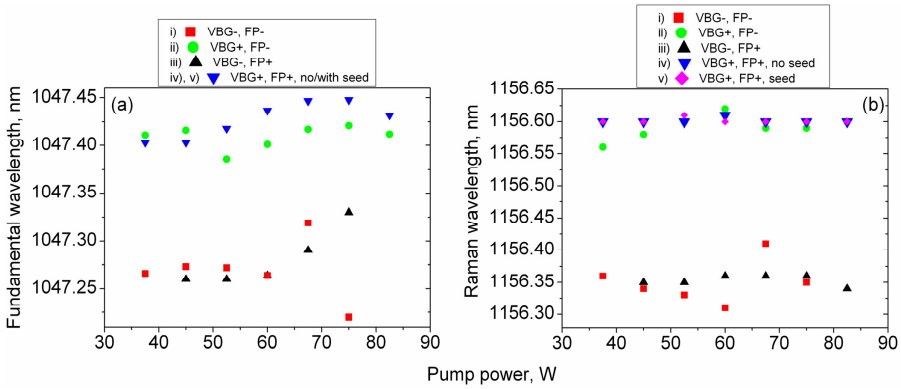

Fig. 5. (a) Fundamental and (b) Raman lasers wavelengths as functions of incident diode pump power for the different cavity configurations.

The wavelengths of the fundamental laser for the different configurations are shown in Fig. 5(a). The fundamental wavelength varied by 0.04-0.06 nm around the average value of ~1047.28 nm without the VBG and at ~1047.42 nm with the VBG element. The presence of the VBG in the fundamental laser cavity (configuration ii)) does not stabilize the Raman wavelength either, as can be seen from Fig. 5(b), and the magnitude of the variation with the pump power was similar with and without the VBG (configuration i)). The only difference is the average wavelength: ~1156.35 nm for configuration i) and ~1156.6 for configuration ii), set by the Raman shift of the VBG defined fundamental wavelength. In all cases the Stokes shift between the fundamental and Raman wavelengths was ~901 cm^{-1}. Improved stabilization of the Raman laser wavelength (0.01 nm around the average value of 1156.6 nm) is observed when the etalon (FP) is inserted into the Raman laser cavity (configurations ii)-v)), see Fig. 5(b).

The pulse duration of the Raman laser output did not depend on the configuration, decreasing from 36 to 32 ns as the incident pump power increased from 35 to 85 W.

4. Discussion

The presence of the VBG in the fundamental laser cavity moves the emission peak towards longer wavelengths, as shown in Fig. 5(a). The gain bandwidth in Nd:YLF crystal is ~1.35 nm [25,26]. Therefore, it may be that the pulse energy at 1047 nm is lower with the VBG in the cavity due to a shift of the laser emission wavelength away from the Nd:YLF gain peak. Besides, the lower reflectivity of the VBG element (99.9% at 1047 nm) compared to the HR mirror (<99.99%) is likely to have further decreased the intracavity pulse energy at 1047 nm wavelength. Lower pulse energy at 1047 nm for the same pump power is the main reason why the Raman laser threshold of 35 W in configuration ii) is higher than that in configuration i) (26 W), i.e. without VBG [Fig. 3(a)]. The slope efficiency of the Raman laser, nevertheless, remains the same (3.3%) as it is mainly determined by the Raman laser output coupler reflectivity and passive losses in the Raman cavity [27]. This in turn explains the slightly lower slope efficiency of 3% and higher threshold (36 W) for the Raman laser in

#216576 - $15.00 USD Received 7 Jul 2014; revised 15 Aug 2014; accepted 17 Aug 2014; published 2 Sep 2014

configuration iii) (VBG-, FP +), where the FP filter introduces additional losses to the Raman cavity. On the other hand, the fundamental cavity did not contain the VBG element in this case but the Raman threshold was ~38% higher than that in the case of configuration i) (VBG-, FP-). This can be explained in addition by the stabilization of the Raman laser wavelength by the FP filter (see Fig. 5(b), black triangles), while the fundamental wavelength changes with the pump power (see Fig. 5(a), black triangles), thus inducing a reduction in the Raman gain in the Raman laser due to the mismatch of the fundamental and Raman wavelengths.

The lower Raman laser slope efficiency of 2.4% for configurations iv) and v) (i.e. VBG + , FP + , with and without injection seeding) can be explained by the combined effect of the linewidth narrowing elements in both fundamental (VBG) and Raman (FP) cavities. The VBG reduces the intracavity pulse energy at the fundamental wavelength of 1047 nm, thus reducing the overall Raman gain in the Raman laser (which is a product of the Raman gain, pump intensity and the Raman crystal length [28]), while FP filter in the Raman cavity introduces additional losses for the Raman emission, similar to the configuration iii). The lower threshold of the Raman laser (33 W) in configuration v) (VBG + , FP + with injection seeding) compared to configuration iv) without seeding (35 W) results from the fact that the Raman field need no longer build up from noise [28]. Without the seed, the Raman noise originates from the spontaneous Raman scattering and its intensity is significantly lower than that of the seed.

The higher stability of the Raman wavelength in the configurations with the FP etalon (0.01-0.02 nm) in comparison with that without the etalon and only with the VBG in the fundamental laser cavity (0.06 nm), Fig. 5(b), can be explained by the narrower filter function of the FP than that of the VBG, and the higher sensitivity of the Raman laser to losses due to lower gain in comparison with the fundamental laser.

The theory of SRS [29,30] predicts that in the case of a single-mode (monochromatic) fundamental, where the fundamental linewidth is significantly narrower than the spontaneous Raman linewidth of a crystal (i.e. tends to zero), one should observe so-called gain-narrowing of the Raman laser linewidth with respect to the spontaneous Raman linewidth. This narrowing is inversely proportional to the square root of the fundamental intensity and can be as high as 6 at the threshold for SRS [28, 29, 31]. In contrast, when the fundamental linewidth is significantly broader than the spontaneous Raman linewidth of a crystal, the linewidth of the Stokes emission of the Raman laser will tend to be as broad as that of the fundamental [30].

The latter case can be illustrated by a practical example [32] where intracavity pumping of a $BaWO_4$ Raman crystal (with the narrow Raman linewidth of 1.6 cm^{-1}) with a fundamental laser of linewidth of 1.77 cm^{-1} led to a Raman laser emission linewidth of 1.12 cm^{-1} at the Raman threshold (increasing to 3.74 cm^{-1} at higher pump powers).

The present experimental research deals with the intermediate case, when the pump linewidth is not significantly narrower than the Raman linewidth (which is 5.4 cm^{-1} in KGW crystal at 901 cm^{-1} Raman frequency [33]). Experimental data indicate that in this case, when no special narrowing elements are put in both fundamental and Raman laser cavities, the Raman laser emission linewidth at Raman threshold is close to that of the fundamental emission [Fig. 4 (a)] similar to experimental results in [32]. Separate insertion of the emission linewidth narrowing element into either only the fundamental laser cavity or only the Raman laser cavity, in case of a KGW crystal, does not lead to any substantial narrowing of the Raman emission linewidth, especially at pump powers above the threshold [Fig. 3(b)]. The mechanism which allows the Raman laser linewidth to broaden in the presence of a broadband pump emission despite the presence of the FP etalon in the Raman cavity at high pump powers could be due to the broadening of the effective double-pass transmittance spectrum of the FP etalon [Fig. 1(b)]. This broadening will happen when the Raman laser starts to oscillate in multi-transverse mode regime at high pump powers, thus leading to increased angle of incident of the Raman beam into the FP etalon due to the increased

#216576 - $15.00 USD Received 7 Jul 2014; revised 15 Aug 2014; accepted 17 Aug 2014; published 2 Sep 2014

divergence of the Raman laser beam. Raman laser could then oscillate on adjacent etalon modes, corresponding to different angles of incident to the FP filter, which results in broadening of the Raman emission.

In the case of a KGW Raman crystal one should aim for linewidth narrowing elements being put into both fundamental and Raman laser cavities in order to observe substantial narrowing of the Raman laser emission, even at high pump powers. Locking of the Raman resonator oscillation frequency to that of the seed laser by controlling the resonator length would significantly narrow the Raman laser emission further.

5. Conclusion

The use of an N_g-cut KGW crystal in an intracavity pumped pulsed Raman laser was demonstrated. The peak power of the pulses was 20 kW and the emission linewidth was narrowed to 0.43 cm^{-1} at 1156 nm using linewidth narrowing elements in both the fundamental and Raman cavities as well as injection seeding of the Raman resonator. Linewidth narrowing of the Raman emission was studied for different configurations of both the fundamental and Raman cavities. The analysis performed shows that narrow linewidth emission in an intracavity pumped Raman laser can be achieved efficiently by the combination of narrow linewidth pump source and linewidth narrowing elements in the Raman laser cavity. Injection seeding of Raman cavity was shown to be an effective tool for further linewidth narrowing in pulsed Raman lasers analogous to solid-state ones.

Acknowledgments

The author gratefully acknowledges Professor Alan J. Kemp for fruitful discussions. This works was funded in part by the European Research Council (ERC; 278389).

#216576 - $15.00 USD Received 7 Jul 2014; revised 15 Aug 2014; accepted 17 Aug 2014; published 2 Sep 2014